

The effects of strain rate and soil remolding on uplift response of buried submarine pipelines

Santiram Chatterjee¹, S. Maitra¹, and D. Choudhury¹

¹ Department of Civil Engineering, Indian Institute of Technology Bombay, Powai, Mumbai – 400076, India.

ABSTRACT

Buried submarine pipelines are key components of offshore hydrocarbon extraction facilities. These pipes carry oil and gas maintained at high internal temperature and pressure. The thermal stresses developed because of temperature differences between laying and operational phases of these pipes may subject them to buckling. Several researchers have studied the soil response when the pipe undergoes upheaval buckling. However, the existing design methodologies do not consider the effects of strain rate and soil remolding on undrained shear strength of soil and its consequential effect on uplift capacity. In the present study, the effects of strain rate and remolding on uplift response of buried pipes are studied. The large deformation finite element approach has been used to model pipe-soil interactions for different values of strain rate parameter, pipe velocity, soil sensitivity, pipe embedment and soil unit weight. It is seen that the effects of strain rate on uplift capacity may be significant and a model is proposed that can quantify these effects. On the other hand, soil remolding is found not to affect the peak uplift resistance significantly as peak resistance is mobilized at relatively small pipe displacements.

Keywords: buried pipes; upheaval buckling; large deformation finite element modelling; strain rate; soil remolding

1 INTRODUCTION

Submarine pipelines are used for conveyance of hydrocarbons in offshore oil and gas production facilities and are subjected to high internal temperature and pressure. At deep water locations, offshore pipes are generally laid on the seabed (on-bottom pipelines), whereas, at nearshore shallow water regions, the pipes are generally buried into the seabed. Pipeline burial protects the pipe from hydrodynamic wave forces and also provides thermal insulation which ensures smooth fluid flow within the pipe. The thermal stresses developed due to temperature differences between laying and operational phases of these pipes may subject them to upheaval buckling. The soil cover above the pipe provides resistance to this buckling.

The uplift mechanisms are broadly classified into local and global soil failure mode (DNV 2017). In the local soil failure mode, the mechanism is similar to that of a deeply embedded pile subjected to lateral loading (Randolph and Houlsby 1984). For buried pipes, this mechanism involves a local flow of soil with slip planes extending from top to bottom of the pipe. The uplift capacity factors under such cases in weightless soil are $(6 + \pi)$ and $(4\sqrt{2} + 2\pi)$ for perfectly smooth and rough pipe-soil interface respectively. In the global soil failure mode, soil lying above the pipe is lifted upwards resulting in a failure mechanism reaching the mudline. Martin and White (2012) carried out an extensive study on the various factors influencing undrained bearing capacity for offshore pipes. Prediction models for

estimating undrained uplift capacity of buried pipes have been proposed by Maitra et al. (2016) and Maitra et al. (2017). The drawbacks of the current DNV guidelines for estimation of uplift capacity have been highlighted in these studies. From these studies, the various factors influencing uplift capacity can be categorized into the following groups: (a) pipe parameters: diameter (D), invert embedment (w); (b) soil parameters: undrained shear strength (s_u) profile, buoyant unit weight (γ'); and (c) pipe-soil interface parameters: interface tension (T), interface roughness (α).

During pipe buckling, the soil mass surrounding these pipes are often subjected to varying levels of strain rates and also may undergo remolding which may alter the shear strength of soil. Chatterjee et al. (2012) and Ghorai and Chatterjee (2017) have studied the effects of strain rate and soil remolding on pipe-soil interactions for on-bottom pipes. However, these aspects have not been considered by earlier researchers for studying uplift response of buried pipes. In the present paper, the effects of strain rate and remolding are studied using large deformation finite element (LDFE) methodology in which s_u of soil is modified after every small incremental displacements of pipe. Finally, the design methodology proposed by Maitra et al. (2016) is modified which now incorporates the effects of strain rate on undrained uplift capacity.

2 NUMERICAL METHODOLOGY

A two-dimensional plane strain finite element (FE) model was constructed using commercial FE package Abaqus. Mesh was discretized using six-noded quadratic triangular elements. Fig. 1 shows an example of FE mesh for embedment ratio (w/D) of 2. The LDFF approach has been used to model pipe-soil interactions in which the overall pipe displacement is discretized into a series of small incremental displacements (2% of D) and small strain FE analyses are carried out for each increment. After each small strain analysis, a new mesh is constructed for the deformed problem domain and stresses, strains and other field variables are interpolated from the old mesh to the new one using “Remeshing and Interpolation Technique with Small Strain” (RITSS) (Hu and Randolph 1998a and 1998b).

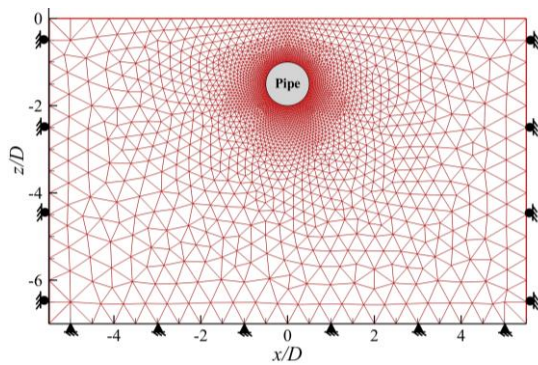


Fig. 1. Finite element mesh modelled in Abaqus for $w/D = 2$

The pipe is modelled as rigid and weightless and a smooth pipe-soil interface is assumed. Various values of w/D and normalized buoyant unit weight of soil ($\gamma'D/s_u$) have been considered (γ' and s_u have been assumed to be unvarying along depth). Extreme values of interface tension ($T = 0$ and ∞) have been considered here. $T = 0$ signifies “No Tension” (NT) conditions in which separation is allowed at pipe-soil interface, whereas, for modelling $T = \infty$ (“Full Tension” (FT)), separation is restricted at interface.

The soil is modelled as linearly elastic perfectly plastic material (i.e., Tresca constitutive relationship) with a Poisson’s ratio of 0.499 (≈ 0.5) and a deformation modulus of $500s_u$. In order to incorporate the effects of strain rate and remolding on s_u , the Tresca material response has been modified using the approach suggested by Einav and Randolph (2005) and Zhou and Randolph (2007). The undrained shear strength of soil is expressed as:

$$s_u = s_{u0} \left[1 + \mu \log \left\{ \max(\dot{\gamma}_{\max}, \dot{\gamma}_{\text{ref}}) / \dot{\gamma}_{\text{ref}} \right\} \right] \times \left[\delta_{\text{rem}} + (1 - \delta_{\text{rem}}) \exp(-3\xi / \xi_{95}) \right] \quad (1)$$

Using Eq. (1), s_u is modified after each incremental displacement and thus, the combined effects of strain rate and remolding on original shear strength (s_{u0}) are incorporated. The influence of strain rate $\dot{\gamma}$ is

expressed in the first part of the equation where $\dot{\gamma}_{\text{ref}}$ is the reference shear strain rate (generally taken as 1% per hour $\sim 3 \times 10^{-6} \text{ s}^{-1}$). The rate parameter μ signifies the rate of increase of s_u per decade and lies typically in the range of 0.05-0.20 (Biscontin and Pestena 2001). $\dot{\gamma}_{\max}$ is the maximum rate of shear strain and is expressed as:

$$\dot{\gamma}_{\max} = \frac{\Delta \varepsilon_1 - \Delta \varepsilon_3}{\delta / D} \frac{v}{D} \quad (2)$$

In Eq. (2), $\Delta \varepsilon_1$ and $\Delta \varepsilon_3$ are the major and minor principal strains respectively; v is the pipe velocity and δ is the incremental displacement applied in each step of LDFF. The second part of Eq. (1) captures the effects of remolding on s_u . δ_{rem} is the inverse of soil sensitivity (S_t) and ξ is the cumulative plastic shear strain. ξ_{95} is the magnitude of ξ corresponding to 95% remolding and has a range of 10-50 (Randolph 2004). ξ_{95} is assumed to be 20 in the present study.

μ and S_t were varied over wide ranges to study their effects on uplift response. Initially the effects of strain rate and remolding are studied separately and in later part, their combined effects are studied. The pipe was subjected to uplift at various pull-out rates expressed non-dimensionally as $v/D \dot{\gamma}_{\text{ref}}$. Table 1 shows a list of input parameters considered in the present study.

Table 1. List of input parameters for study of strain rate and remolding effects on buried pipe-soil interaction

Category	μ	$v/D \dot{\gamma}_{\text{ref}}$	S_t	w/D	$\gamma'D/s_u$
Effect of strain rate	0, 0.1, 0.2	$10^1, 10^2, 10^3, 10^4, 10^5$	1	2, 4, 6	0, 2
Effect of soil remolding	0	-	1, 2, 5, 10	2, 4, 6	0, 2
Combined effect of strain rate and soil remolding	0.1, 0.2	$10^1, 10^2, 10^3, 10^4, 10^5$	2, 5, 10	2, 4	0

3 RESULTS AND DISCUSSIONS

3.1 Effects of strain rate

In this section, the effects of strain rate are studied in isolation (S_t is assumed to be 1). Fig. 2 shows an example of uplift resistance (V) versus pipe displacement (δ) plot at various pullout rates for $\mu = 0.1$ and $w/D = 2$ in weightless soils under NT conditions. $V - \delta$ plot for $\mu = 0$ is also included in the figure for comparative purpose. The figure shows that uplift resistance can increase significantly with increase in pipe velocity. Similar plots were obtained for various values of w/D and T . From these plots, uplift capacity (V_u) which is essentially the peak uplift resistance is obtained and correspondingly the uplift capacity factors ($V_u/s_u D$) for various w/D , T and $\gamma'D/s_u$ are determined. Fig. 3 shows the obtained values of $V_u/s_u D$ in

weightless soil. It can be seen that $V_u/s_u D$ increases linearly with logarithm of $v/D\dot{\gamma}_{ref}$. This increase in capacity is due to the viscous behavior of soil playing a role in increase of s_u at higher pullout rates. Fig. 4 shows some examples of failure mechanisms which illustrates the transition in mechanism from shallow mode to deep failure mode with increase in embedment.

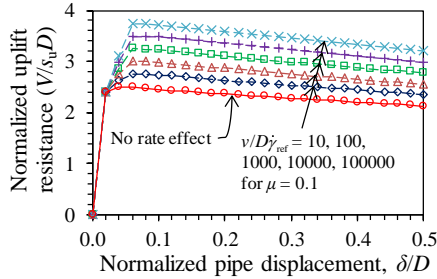


Fig. 2. Comparison of $V/s_u D$ at various pullout rates for $\mu = 0.1$ with $\mu = 0$ for $w/D = 2$, $T = 0$ and $\gamma'D/s_u = 0$

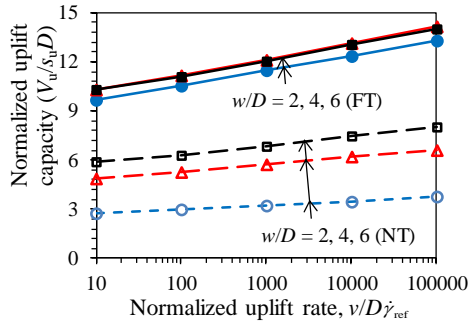


Fig. 3. $V_u/s_u D$ at various uplift rates for $w/D = 2, 4$ and 6 ; $T = 0$ and ∞ ; and $\gamma'D/s_u = 0$

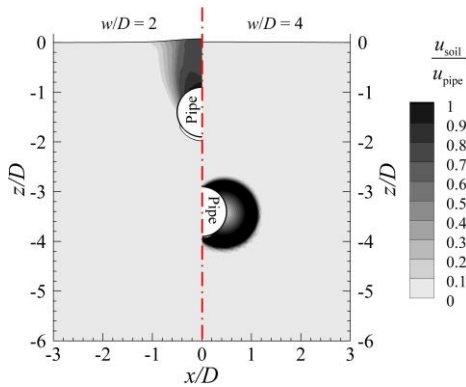


Fig. 4. Uplift mechanisms for $w/D = 2$ and 4 , $\gamma'D/s_u = 2$ under NT conditions ($\mu = 0.2$, $v/D\dot{\gamma}_{ref} = 1000$)

The effects of strain rate on soil response have been quantified for on-bottom pipelines by previous researchers using a factor f_r (Chatterjee et al. 2012; Ghorai and Chatterjee 2017). Similar approach can be applied for buried pipes as well. The operative (or an equivalent) shear strength $s_{u,eq}$ is expressed as:

$$s_{u,eq} = s_{u0} \left[1 + \mu \log \left\{ \max \left(1, f_r v / D\dot{\gamma}_{ref} \right) \right\} \right] \quad (3)$$

The factor f_r was varied to bring various curves together in Fig. 2 and other similar plots. $f_r = 0.9$ was found to be appropriate for all cases. The various curves in Fig. 2 reduce to a narrow band when V is normalized with respect to $s_{u,eq} D$ (see Fig. 5(a)). As a result of this, $V_u/s_{u,eq} D$ becomes independent of $v/D\dot{\gamma}_{ref}$ (see Fig. 5(b)). The obtained values of $V_u/s_{u,eq} D$ matches with the uplift capacity factors proposed by Maitra et al. (2016) in which rate effects were not considered. Thus, Eq. (3) can be combined with the design methodology proposed by Maitra et al. (2018) to incorporate the effects of strain rates on uplift capacity. V_u is obtained numerically for various sets of parameters listed in Table 1 and is compared with V_u estimated using the proposed model. It was seen that average absolute error was 3.8% for assumed set of parameters and thus the proposed model is able to quantify the effects of strain rates reasonably well.

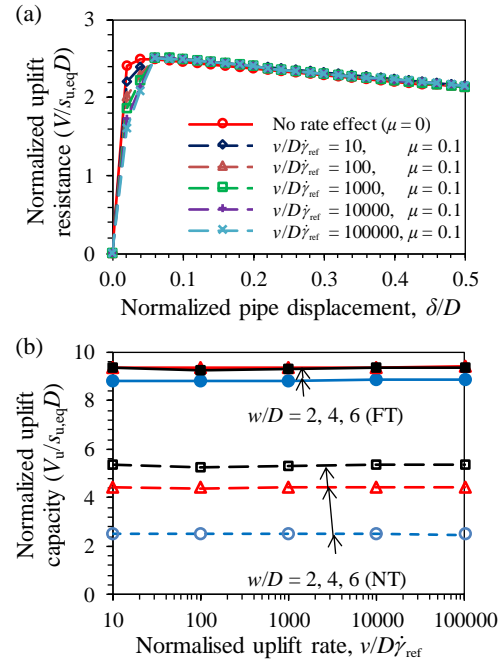


Fig. 5. (a) Uplift resistance, V normalized with $s_{u,eq} D$ for $w/D = 2$, $T = 0$ and $\gamma'D/s_u = 0$; (b) Uplift capacity, V_u normalized with $s_{u,eq} D$ for $w/D = 2, 4$ and 6 ; $T = 0$ and ∞ ; and $\gamma'D/s_u = 0$

3.2 Effects of soil remolding

In this section, the effect of soil remolding is studied in isolation (μ was assumed to be 0). The uplift capacity for various cases of S_t , w/D , $\gamma'D/s_u$ and T were obtained. Fig. 6 shows an example of uplift resistance – pipe displacement plot for $w/D = 2$ and $\gamma'D/s_u = 0$. The figure shows that V_u is not significantly influenced by soil sensitivity as peak uplift resistance is mobilized at small magnitudes of strain i.e., before any significant soil remolding occurs. For various parameters listed in Table 1, V_u is found to change by less than 1% for change in S_t from 1 to 10 and thus, the effect of soil sensitivity on V_u can be neglected for all practical

purposes. However, sensitivity influences the post-peak response as major remolding occurs only after relatively larger pipe displacement.

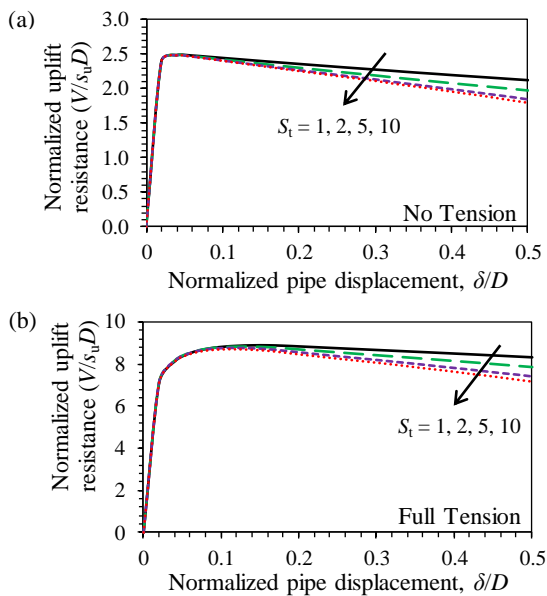


Fig. 6. $V/s_u D$ for $S_t = 1, 2, 5$ and 10 ; $w/D = 2$; and $\gamma' D/s_u = 0$ under (a) No Tension; (b) Full Tension conditions

3.3 Combined effects of strain rate and soil remolding

Several combinations of μ (> 0), $v/D \dot{\gamma}_{ref}$ and S_t (> 1) were considered (see Table 1) and analyses were carried out for these set of parameters to study the combined influence of strain rate and soil remolding on uplift response. Fig. 7 shows an example of uplift resistance (V) - pipe displacement (δ) plot at various pullout rates for $\mu = 0.1$, $S_t = 10$ and $w/D = 2$ in weightless soils under NT conditions. Since V_u is found to be independent of S_t (see section 3.2), the peak uplift resistance for all pullout rates in Fig. 7 are identical to that of Fig. 2. However, after peak resistance is mobilized, the decrease in uplift resistance as the pipe undergoes uplift is more for soils with higher values of s_t because of combined effects of soil remolding and loss in embedment during uplift (post-peak uplift resistance in Fig. 7 is less than that of Fig. 2).

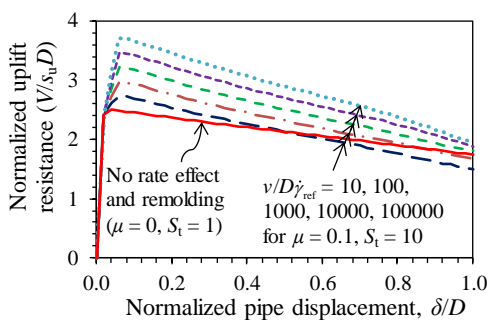


Fig. 7. Comparison of $V/s_u D$ at various pullout rates for $\mu = 0.1$, $S_t = 10$ with $\mu = 0$, $S_t = 1$ ($w/D = 2$, $T = 0$ and $\gamma' D/s_u = 0$)

4 CONCLUSIONS

In the present study, the effects of strain rate and soil remolding on uplift response of buried pipes are studied. It has been found that uplift resistance can increase significantly with increase in strain rate because of viscous behavior of soil. This increase in uplift resistance with increase in pullout rate is quantified using a model that considers the change in s_u corresponding to various uplift rates. Several values of soil sensitivity were also considered and it has been found that soil remolding has negligible effect on uplift capacity as peak resistance is mobilized at small pipe displacements. However, the soil resistance at larger displacements are found to depend on soil sensitivity.

REFERENCES

- Biscontin, G., and Pestana, J.M. (2001). Influence of peripheral velocity on vane shear strength of an artificial clay. *Geotechnical Testing Journal*, 24(4), 423–429.
- Chatterjee, S., Randolph, M.F., and White, D.J. (2012). The effects of penetration rate and strain softening on the vertical penetration resistance of seabed pipelines. *Géotechnique*, 62(7), 573–582.
- DNV (2017). DNV-RP-F114: Pipe-soil interaction for submarine pipelines, Det Norske Veritas (DNV), Oslo, Norway.
- Einav, I., and Randolph, M.F. (2005). Combining upper bound and strain path methods for evaluating penetration resistance. *International Journal for Numerical Methods in Engineering*, 63(14), 1991–2016.
- Ghorai, B., and Chatterjee, S. (2017). Influences of strain rate and soil remoulding on initial break-out resistance of deepwater on-bottom pipelines. *Computers and Geotechnics*, 91, 82–92.
- Hu, Y., and Randolph, M.F. (1998a). A practical numerical approach for large deformation problems in soil. *International Journal for Numerical and Analytical Methods in Geomechanics*, 22(5), 327–350.
- Hu, Y., and Randolph, M.F. (1998b). H-adaptive FE analysis of elasto-plastic nonhomogeneous soil with large deformation. *Computers and Geotechnics*, 23(1–2), 61–83.
- Maitra, S., Chatterjee, S., and Choudhury, D. (2016). Generalized framework to predict undrained uplift capacity of buried offshore pipelines. *Canadian Geotechnical Journal*, 53(11), 1841–1852.
- Maitra, S., Chatterjee, S., and Choudhury, D. (2017). Effect of pipe-soil interface roughness on undrained uplift capacity of buried offshore pipelines. *Proc., The 27th International Ocean and Polar Engineering Conference, International Society of Offshore and Polar Engineers, San Francisco*.
- Martin, C.M., and White, D.J. (2012). Limit analysis of the undrained bearing capacity of offshore pipelines. *Géotechnique*, 62(9), 847–863.
- Randolph, M.F., and Houlsby, G.T. (1984). The limiting pressure on a circular pile loaded laterally in cohesive soil. *Géotechnique*, 34(4), 613–623.
- Randolph, M.F. (2004). Characterization of soft sediments for offshore applications. Keynote paper, *Proc., 2nd Int. Conf. on site characterization, Porto, Portugal*, 209–231.
- Zhou, H., and Randolph, M.F. (2007). Computational techniques and shear band development for cylindrical and spherical penetrometers in strain-softening clay. *International Journal of Geomechanics*, 7(4), 287–295.